Assessing Changes of Water Yield in Qinghai Lake Watershed of China

Xi-hong Lian [1,2], Yuan Qi [1,*], Hong-wei Wang [1], Jin-long Zhang [1] and Rui Yang [1,2]

[1]   Key Laboratory of Remote Sensing of Gansu Province, Northwest Institute of Eco-Environment and Resources, Chinese Academy of Sciences, Lanzhou 730000, China; lianxh@lzb.ac.cn (X.-h.L.); wanghw@lzb.ac.cn (H.-w.W.); zjinlong@lzb.ac.cn (J.-l.Z.); yangrui@lzb.ac.cn (R.Y.)

[2]   University of Chinese Academy of Sciences, Beijing 100049, China

*   Correspondence: qiyuan@lzb.ac.cn

Abstract: Water yield is an important ecosystem service, which is directly related to human welfare and affects the sustainable development. Using the integrated valuation of environmental services and tradeoffs model (InVEST model), we simulated the dynamic change of water yield in Qinghai lake watershed, Qinghai, China, and verified the simulation results. This paper emphatically explored how precipitation change and land use/land cover change (LUCC) affected the change of water yield on the spatial and temporal scales. Before 2004, the areas of cultivated land and unused land showed a dramatic increasing tendency, while forestland and water area presented a decreasing trend. After 2004 cultivated land changed slowly, unused land decreased. Grassland revealed a general trend of decline during 1977–2018, while built-up land basically presented a linear increase. The results show that water yield fluctuated and increased during 1977–2018. From 1977 to 2000, the mean water yield in each sub-watershed showed an increasing trend and afterward a decreasing one. After 2000, the sub-watersheds basically showed an increasing tendency. There was a strong correlation, with a correlation coefficient of 0.954 ** (** correlation is significant at the 0.01 level), between precipitation and water yield. Land use/land cover change can change the hydrological state of infiltration, evapotranspiration, and water retention. Meanwhile, the correlation between built-up land and water yield was the highest, with a correlation coefficient of 0.932, followed by forestland, with a correlation coefficient of 0.897. Through the analysis of different scenarios, we found that compared with land use/land cover change, precipitation played a more dominant role in affecting water yield.

Keywords: water yield; InVEST model; LUCC; climate change; Qinghai Lake

1. Introduction

Ecosystem services, which represent the benefits that human beings derive from ecosystem, are related to socioeconomic development and human wellbeing [1,2]. Ecosystem services include provisioning, regulatory, supporting, and cultural services [3,4]. Many ecosystem services are crucial for human survival, especially the water-related ecosystem services [5,6], such as water yield, which plays a basic role in agriculture, industry, and quality of life for humans [7,8]. Abundant water provision means the sustainable development of the regional economy and society. Quantitative evaluation and visualization of water yield is helpful to understand the trends of water supply function of ecosystem, and is beneficial to reveal the relationship between human beings and water resources, which is of great significance for scientific management and utilization of water resources [9].

Models play a significant role in assessment of water yield, because they can estimate and simulate the spatial distribution of water yield [10]. However, more and more attention has been paid to the

accuracy of the model output and the validation and evaluation of the performance of models in different circumstances and locations [11,12]. The input parameters have a great influence on the output results of the model. Many studies use sensitivity analysis methods to analyze the dependence between model output and variables [13,14], and in turn adjust model input parameters to find a set of optimal parameters. In fact, the input parameters of water yield module need to be calculated by physical equation or empirical equation [15,16]. So, we should make the input parameters more reasonable and accurate by standardizing the input data and taking full account of the regional characteristics and differences. In addition, the output results of the model are compared and verified through the observation data to evaluate the performance of the model without sensitive analysis methods and parameter adjustment, so as to provide a supporting evidence for us to use the model in the similar areas without measured data or insufficient data.

Since the 1970s, many distributed hydrological models, including soil and water assessment tool (SWAT) [17], artificial intelligence for ecosystem services (ARIES) [18], integrated valuation of ecosystem services and tradeoffs (InVEST) [19] and so on, have been established. Each model has advantages and disadvantages. However, in the absence of reliable and readily available datasets, simpler models are potentially more attractive. Compared with SWAT and ARIES, InVEST model has become a popular framework in the analysis of a series of ecosystem services and has been applied in a variety of places [20–22]. As InVEST was designed to deal with long-term average input data, we argue that it is suitable for exploring the long-term effects of LUCC and climate changes on water yield.

Climate change and land use/land cover change (LUCC) caused by human activities are the most important factors for change of water yield [23]. Climate change which regulates water supply on a macro scale, can alter the water yield by changing the precipitation and potential evapotranspiration in a watershed [24,25]. The water yield may change because of human-induced land use [26,27]. Previous studies have explored the effects of land use changes on spatial and temporal variations in water yield [28–30]. The land use data they used were only the results of the primary classification. In fact, the effect of land use change on water yield is very complicated [31]. Different land use conversions are not same on water yield. Little attention has been given to using more detailed classification criteria, especially in long time series. Therefore, it is necessary to explore how these two factors affect the changes of water yield in study area. Understanding underlying mechanisms of driving factors to water yield is the ultimate goal of our simulation and evaluation. Previous studies elucidate the driving mechanisms by using scenario simulations and calculating contribution rates [32]. There are few studies on quantitative evaluation of water yield ability of different types of LUCC. It is significant to quantify individual LUCC type to water yield, because it is not only crucial to analysis, also useful to improving the predictability of water yield dynamic response to LUCC [33].

In this study, we selected the Qinghai lake watershed as the study area, and analyzed the changes of water yield because of the climate change and LUCC. The performance of the integrated valuation of environmental services and tradeoffs (InVEST) water yield models was assessed in Qinghai lake watershed. The primary aim of this paper is to provide foundation for scientific management of water resources. The specific objectives of this study are to: (1) Assess the dynamic change of water yield over the period of 1977 to 2018; (2) verify the model results by observation data; (3) reveal the dynamic relationship between water yield change and precipitation and LUCC, especially specific to individual LUCC type; (4) evaluate the applicability of the InVEST model in Qinghai lake watershed and provide reference information for water resource management and ecological protection.

2. Materials and Methods

2.1. Study Area

Qinghai lake watershed (Figure 1) is located in the northeast of Qinghai-Tibet Plateau, China between 36°15′–38°20′ N and 97°50′–101°20′ E, and covers an area of approximately 29,646 km². Qinghai lake is the largest inland saline lake in China. Qinghai lake watershed is a natural barrier to

prevent the west from desert spreading from the east, and is an important node to maintain ecological security in the northeast of Qinghai-Tibet Plateau [34,35]. In general, the temperature increases from northwest to southeast in the watershed. The watershed has a typical plateau continental climate with average annual temperatures of about −0.7 °C and a mean annual precipitation of 381 mm [36,37]. The topography of the watershed decreases from the northwest to the southeast. There are three main vegetation types in the study area, they are Potentilla fruticosa shrub, Kobresia meadow, and Achnatherum splendens steppe. The ecological environment of Qinghai lake watershed largely reflects the overall ecological change trend of Qinghai-Tibet plateau. Because of its unique geographical location and environment, the watershed has become an ecologically fragile area.
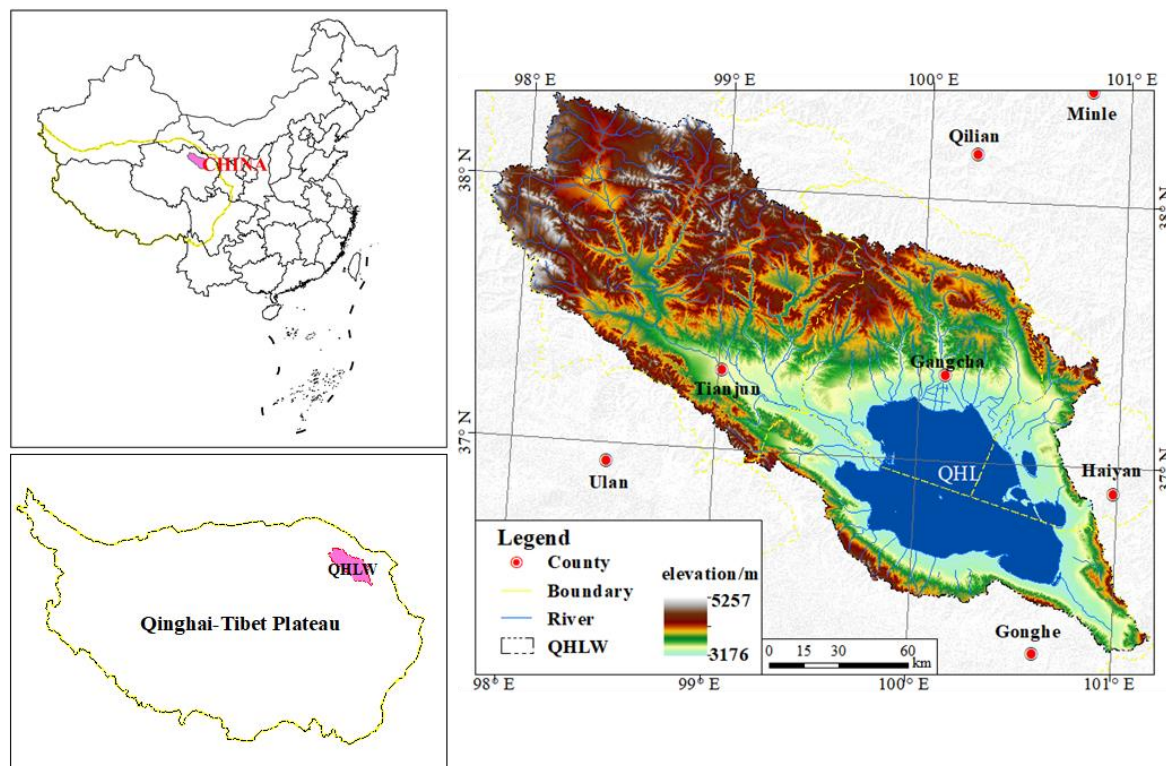

Figure 1. Location of Qinghai lake watershed.

2.2. Water Yield Module

The InVEST model was developed in 2007 by Stanford University, the World Wildlife Fund for Nature and the Nature Conservancy to assess the ecosystem services and support environmental decision-making. The water yield module in the InVEST model is based on the Budyko curve and the annual average precipitation [38,39]. The model algorithm is as follows:

$$Y_x = (1 - \frac{AET_x}{P_x}) \times P_x \tag{1}$$

where Y_x is the water yield of pixel x, AET_x is the annual actual evapotranspiration for pixel x, and P_x is the annual precipitation on pixel x. $\frac{AET_x}{P_x}$ approximates the Budyko curve [40].

$$\frac{AET_x}{P_x} = 1 + \frac{PET_x}{P_x} - \left[1 + \left(\frac{PET_x}{P_x}\right)^\omega\right]^{\frac{1}{\omega}} \tag{2}$$

where PET_x is the potential evapotranspiration for pixel x, ω is the empirical parameter and its expression is:

$$\omega = Z \cdot \frac{AWC_x}{P_x} + 1.25 \tag{3}$$

where AWC_x is the plant available water content and Z is empirical parameter.

Potential evapotranspiration is defined as:

$$PET_x = K_c(\ell_x) \cdot ET_0(x) \tag{4}$$

where $K_c(\ell_x)$ is the plant evapotranspiration coefficient associated with LUCC on pixel, and $ET_0(x)$ is the reference evapotranspiration.

2.3. Data Sources and Preparation

Water yield module requires annual precipitation, average annual reference evapotranspiration, root restricting layer depth, plant available water content (PAWC), LUCC, watersheds, sub-watersheds, biophysical table, and seasonality factor (Z).

The annual precipitation and temperature data were acquired from the China Meteorological Administration. The original data were the daily meteorological observation data of meteorological station and were interpolated into 30 m × 30 m grid data by the Australian National University Splines (ANUSPLIN) package. It should be pointed out that DEM data were used as auxiliary data in the process of meteorological data interpolation. Meteorological stations within and around the Qinghai lake watershed were selected, including 16 stations, such as Tianjun station, Gangcha station, and Haiyan station.

The Penman-Monteith equation is the best equation for estimating ET_0, because it can be used globally without any local calibration [41]. This method is limited in application by the lack of input parameters. With this in mind, Allen suggested to use the Hargreaves equation [42] for estimating ET_0. So in this study, ET_0 is calculated based on the Modified-Hargreaves equation, its expression is:

$$ET_0(x) = CR_a(T_{max} - T_{min})^E \left(\frac{T_{max} + T_{min}}{2} + T \right) \tag{5}$$

where T_{max} and T_{min} are the monthly highest temperature and lowest temperature respectively. R_a is the monthly radiation from the sun's upper atmosphere and is obtained by Allen equation. We used the values of C, E, and T recommended by Hu on the Qing-Tibet plateau [43].

Root restricting layer depth is replaced by reference soil depth as a proxy. *PAWC* is defined as the difference between the fraction of volumetric field capacity and permanent wilting point. Zhou developed a method for *PAWC* estimation using physical and chemical properties of soil [44], its expression is:

$$PAWC = 54.509 - 0.132 \times sand\% - 0.003 \times (sand\%)^2 - 0.055 \times silt\% - 0.006 \times (silt\%)^2 - \\ 0.738 \times clay\% + 0.007 \times (clay\%)^2 - 2.688 \times OM\% + 0.501 \times (OM\%)^2 \tag{6}$$

where *PAWC* is the plant available water fraction; *sand%*, *silt%*, *clay%*, *OM%* are the proportion of sand, silt, clay, and organic matter in soil. The soil data comes from the Harmonized World Soil Database version 1.2 (HWSD) [45]. The data set was provided by Cold and Arid Regions Sciences Data Center at Lanzhou.

The LUCC data included the LUCC data in 1977, 1987, 2000, 2005, 2010, 2018. The first five phases of land use data were interpreted from Landsat Thematic Mapper (TM) and/or Enhanced Thematic Mapper (ETM) images. The last phase of the natural features was interpreted by Landsat ETM images, while the artificial features were interpreted by Gaofen-2 remote sensing images. The LUCC data were classified into 22 classes at 30 m spatial resolution. Considering the difference between the data source of the first five phases and the last phase, we collected the LUCC of Qinghai lake watershed in 2010, which was derived from Data Center for Eco-Environment Protection in the Qinghai Lake Basin, and also obtained the LUCC with spatial resolution of 100 m in 2018, which was taken from the

Data Center of the Chinese Academy of Sciences. Those datasets were used for cross-validation of our interpretation results.

The sub-watersheds data were generated from the 30 m digital elevation model (DEM) by Hydrology Analyst Tools in ArcGIS 10.5. Biophysical table is a table that contains the biophysical coefficients used in water yield module. Each column contains a different attribute. Lucode is the unique code corresponding to each LUCC class. LUCC_desc is to describe the name of each LUCC class. LUCC_veg contains the information on which AET Equation (1) to use. Root_depth is often given as the depth as which 95% of a vegetation type's root biomass occurs. *Kc* is the plant evapotranspiration coefficient for each LUCC class.

Seasonality factor (Z) is an empirical parameter which describes the rainfall intensity and topography characteristics, with typical values ranging from 1 to 30. There are three methods to calculate Z [46]: (i) Using the observed streamflow data; (ii) as a function of the average annual number of rain events; (iii) using global estimations of ω. In our study, we used the third approach to estimate Z, and its expression, that is:

$$Z = \frac{(\omega - 1.25) \cdot P}{AWC} \tag{7}$$

where *P* and *AWC* are the average annual values of precipitation and available water capacity, respectively [8]. According to this method, the calculated Z of the Qinghai lake watershed was equal to 8.5.

We obtained the volume of water yield of Qinghai lake watershed over the years from the Qinghai water resources bulletin, which was published by Qinghai water resources information website.

3. Results

3.1. Dynamic Change of LUCC

LUCC data were divided into 6 level (I) classes and 22 level (II) classes. The interpretation results were verified with the field survey data in 2018, indicating that the overall accuracies of level (I) class and level (II) class were 94.5% and 86.4%, respectively. We compared the results of our interpretation with the collected LUCC data. The results showed that our interpretation was 92% consistent with the published data in 2010. We used field survey data to evaluate the accuracy of published data, and we found that our interpretation accuracy was 5% higher than the data collected in 2018. Meanwhile, it is further explained that different data sources do not affect the final interpretation result.

The mainly land cover types in the Qinghai lake watershed were cultivated land, forestland, grassland, water area, built-up land, and unused land. We divided 22 secondary subcategories under the six primary land types. It can be seen from the spatial distribution of LUCC that the area of grassland coverage was the highest, accounting for approximately 63% of the total area of the watershed. That is to say, the watershed is well covered by vegetation. The area of water area, unused land, forestland, and cultivated land accounted for about 18%, 15%, 1.6%, and 1.5% of the total area, respectively. Forestland is mainly distributed in the Gangcha county. Sandy land is mostly located at the eastern and western parts of Qinghai lake. Wetland is mainly distributed in Tianjun county and Gangcha county. Built-up land is mainly concentrated in the surrounding area of Qinghai lake (Figure 2).

The area of cultivated land increased sharply before 2000 and slowly changed after 2000. The area of cultivated land had increased by 163 km^2 in the past 40 years. From 1977 to 2000, the area of forest land decreased promptly. After 2000, it began to rise. In 2018, the area of forestland was basically the same as that in 1970s. Grassland basically showed a downward trend, which is closely related to regional human activities. Grassland area decreased by 207 km^2 before 2000, and slowly rose from 2000 to 2004. However, it reduced generally after 2004. Before 2004, the water area basically showed a decreasing trend, while, it increased after 2004. Built-up land showed a tendency of linear growth between 1977 and 2018. In particular, built-up area expanded significantly faster from 2010 to 2018. The change in the area of unused land generally increased significantly, then remained stable, and finally decreased sharply (Figure 3).
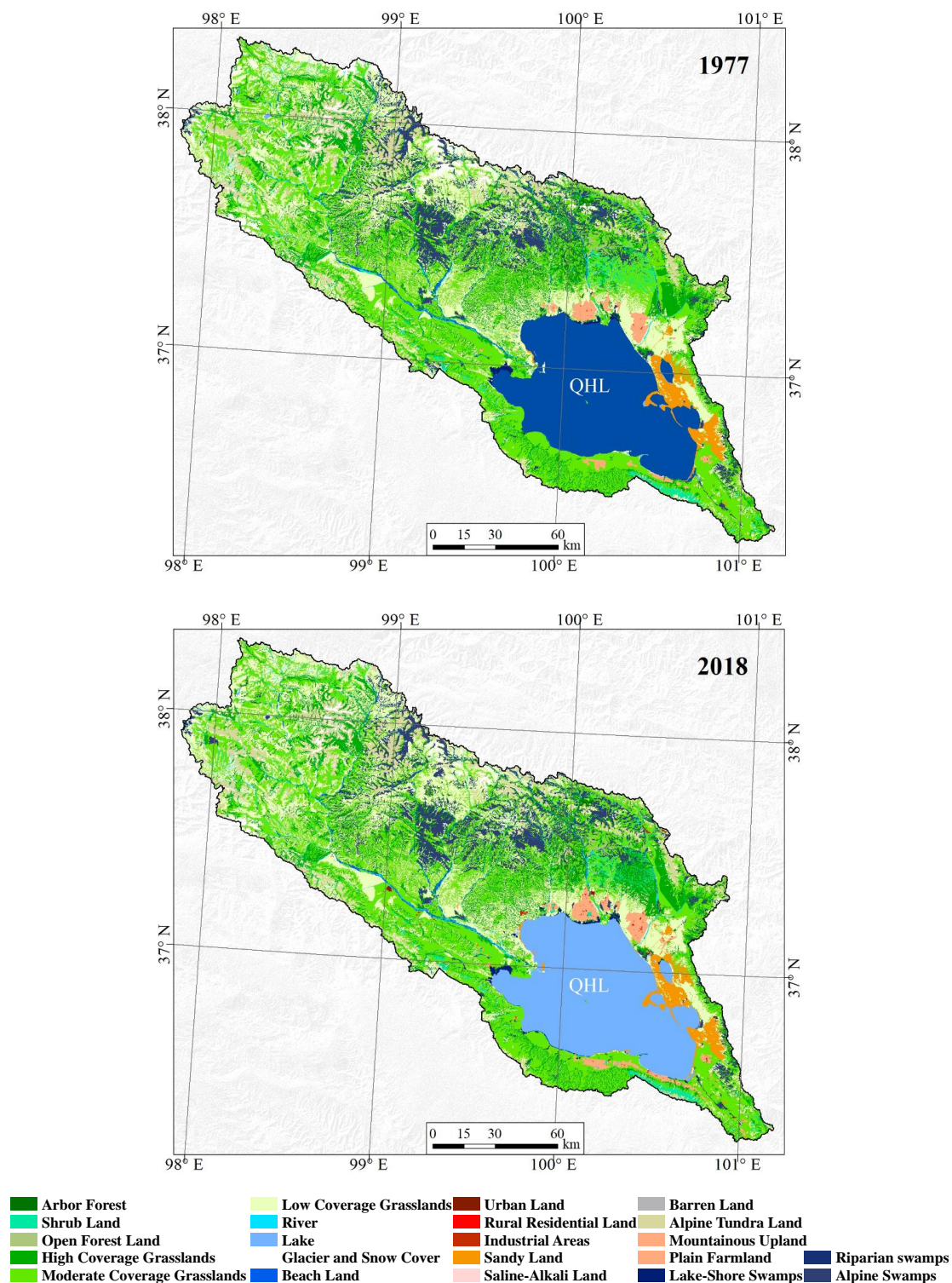
Figure 2. Land use and land cover change (LUCC) patterns in the Qinghai lake watershed.

Taking 1977 as the baseline year, we calculated the land cover change transfer probability matrix of 1987, 2000, 2004, 2010, and 2018. The results indicated that the transformation rules of land types were basically the same in 1987, 2000, 2004, and 2010. The proportion of non-cultivated land conversion from cultivated land was less than 3%. Cultivated land was mostly converted into built-up land, and the proportion had been growing. Forestland was mainly converted into grassland. The percentage of forestland converted to non-forestland increased from 5.47% to 6.72% between 1987

and 2010. Grassland was mostly converted into cultivated land and unused land, and the grassland area remained above 97.76% of the original area. Water area was largely converted into unused land, and proportions of water area were 96.64%, 96.30%, 94.88%, and 95.17% in 1987, 2000, 2004, and 2010, respectively. The percentage of built-up land that had not been transformed into other types of land increased year by year and remained above 99%. Unused land was mainly converted into grassland.
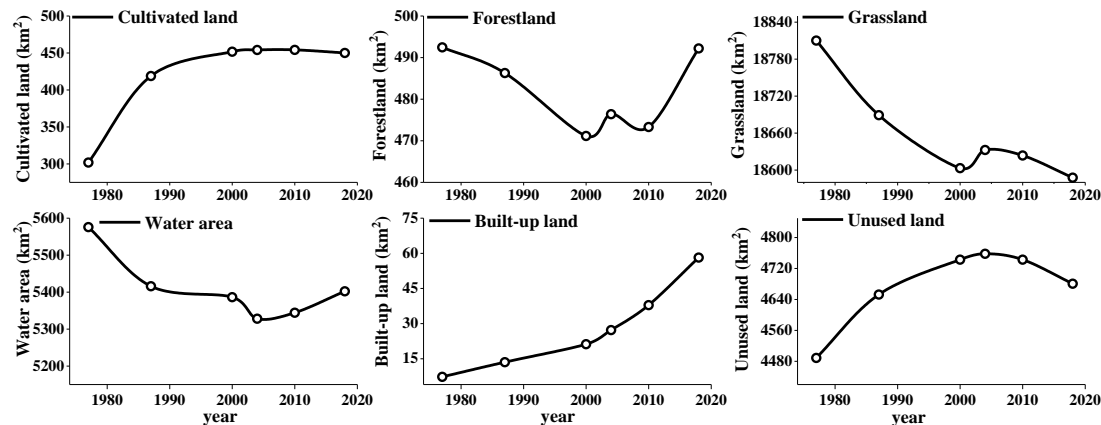

Figure 3. Temporal changes of land use and land cover.

From the transition probability matrix of LUCC during 1977 to 2018, the percentage of cultivated land to forestland, grassland, and built-up land was 3.69%, 2.78%, and 2.81%, respectively. The proportion of forestland to grassland was 8.37%, in addition, there were 2.83% and 0.11% forestland converted to unused land and cultivated land. The proportion of non-grassland conversion from grassland was 3.62%. And 1.80% grassland was converted to unused land, it implied that grassland in these areas had degraded. Water area was basically converted into grassland and unused land, with the proportion of 2.49% and 3.00% respectively. 13.25% of the built-up land was converted to cultivated land, while 1.40% of the built-up land was transformed into grassland. It is notable that 3.54% of built-up land was converted to unused land. The percentage of unused land to grassland and water was 6.08% and 1.11% respectively (Table 1).

Table 1. Transition probability matrix of LUCC during 1977–2018.

Time	LUCC	1977					
		Cultivated Land	Forest Land	Grass Land	Water Area	Built-Up Land	Unused Land
	Cultivated land	90.54%	0.11%	0.93%	0.00%	13.25%	0.03%
	Forestland	3.69%	87.74%	0.18%	0.21%	0.10%	0.07%
2018	Grassland	2.78%	8.37%	96.38%	2.49%	1.40%	6.08%
	Water area	0.02%	0.93%	0.49%	94.28%	0.21%	1.11%
	Built-up land	2.81%	0.02%	0.22%	0.02%	81.50%	0.04%
	Unused land	0.16%	2.83%	1.80%	3.00%	3.54%	92.67%

From 1977 to 2004, the proportion of cultivated land converted to built-up land was 1.8%. An obvious phenomenon was the degradation of forestland into grassland and the transformation of water into unused land (Table 2). From 2004 to 2018, cultivated land was transformed into forestland and grassland. Forestland was transformed into grassland and unused land. The percentage of grassland to water area was the largest. The water area was mainly transformed into grassland and unused land. The proportion of built-up land converted to cultivated land was 10.25%. Unused land was mainly transformed into grassland and water area (Table 3).

Table 2. Transition probability matrix of LUCC during 1977–2004.

Time	LUCC	1977					
		Cultivated Land	**Forest Land**	**Grass Land**	**Water Area**	**Built-up Land**	**Unused Land**
2004	Cultivated land	98.12%	0.00%	0.84%	0.00%	0.47%	0.00%
	Forestland	0.00%	92.85%	0.07%	0.08%	0.00%	0.03%
	Grassland	0.08%	6.41%	97.84%	1.56%	0.17%	2.46%
	Water area	0.00%	0.32%	0.13%	94.88%	0.00%	0.24%
	Built-up land	1.80%	0.01%	0.08%	0.00%	99.36%	0.01%
	Unused land	0.00%	0.40%	1.04%	3.48%	0.00%	97.26%

Table 3. Transition probability matrix of LUCC during 2004–2018.

Time	LUCC	2004					
		Cultivated Land	**Forest Land**	**Grass Land**	**Water Area**	**Built-Up Land**	**Unused Land**
2018	Cultivated land	89.33%	0.11%	0.22%	0.00%	10.25%	0.03%
	Forestland	3.38%	93.59%	0.10%	0.19%	0.21%	0.04%
	Grassland	5.68%	2.58%	98.03%	1.64%	2.24%	4.20%
	Water area	0.02%	0.91%	0.58%	96.19%	0.48%	3.49%
	Built-up land	1.46%	0.01%	0.14%	0.01%	85.00%	0.04%
	Unused land	0.12%	2.80%	0.94%	1.96%	1.82%	92.21%

3.2. Simulation Verification

It should be pointed out that no data were published before 2000, and the water yield data in 2000 refers to the water yield in the surrounding area of Qinghai lake (QHLS). Simulation error was calculated by published data and simulation results. It turned out that simulation errors were 6.93%, 3.45% and 0.26% in 2004, 2010, and 2018, respectively. The year with the largest simulation error was 2004, and the year with the smallest was 2018 (Table 4). Therefore, it can be proved that the InVEST model can be well used to simulate the spatial-temporal change of water yield in Qinghai lake watershed. Meanwhile, it is proved that the input parameters of the model are in accordance with the geographical characteristics of the study area.

Table 4. Actual water yield, simulated results, and simulation error.

Year	Actual_Water Yield/10^8 m^3	InVEST_Water Yield/10^8 m^3	Simulation Error
1977	NAN	18.17	NAN
1987	NAN	23.84	NAN
2000	13.05 (QHLS)	19.03 (QHLW)	—
2004	23.25	24.98	6.93%
2010	29.97	28.97	3.45%
2018	45.57	45.45	0.26%

Note: QHLS refers to the surrounding area of Qinghai lake, and QHLW refers to Qinghai lake watershed.

3.3. Dynamic Change of Water Yield

We focused on the temporal and spatial dynamic changes of water yield in 1977–2018. The results show that water yields tended to increase in Qinghai lake watershed. Volumes of total annual water yield, which were calculated by InVEST model during 1977 to 2018, are showed in Table 2. The lowest water yield value was in 1977, and the highest water yield value was in 2018 (Figure 4). Comparing the water yield and average annual precipitation, we found that two trends were basically the same.
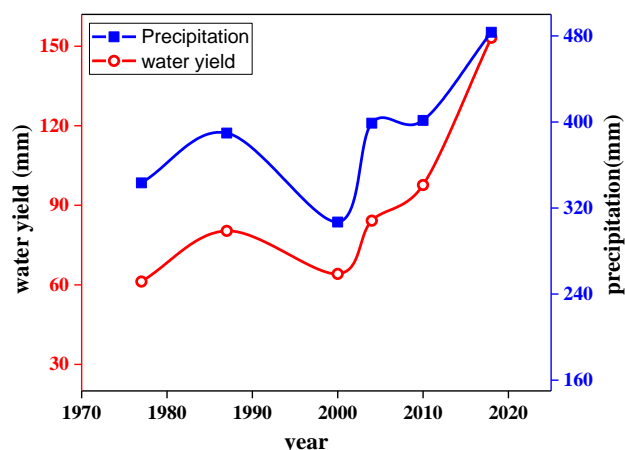
Figure 4. Annual water yields and precipitation of Qinghai lake watershed (1977–2018).

The watershed was delineated into 12 sub-watersheds (Figure 5). We calculated the mean water yield in each sub-watershed. QHL-1 was the largest sub-watershed, which contributed the most to the water yield of Qinghai lake watershed. It should be noted that the mean values of sub-watershed QHL-8 and sub-watershed QHL-9 were close to 0, so no analysis was performed. The lowest mean water yield was sub-watershed QHL-2, and the highest mean water yield was sub-watershed QHL-5. From 1977 to 2000, the mean water yield in each sub-watershed showed an increasing trend and afterward a decreasing one. From 2000 to 2010, sub-watershed QHL-7 and sub-watershed QHL-1 showed a trend of continuous increase, however, sub-watershed QHL-7 showed a decreasing trend from 2010 to 2018. Except for sub-watershed QHL-7, all other sub-watersheds were basically in an increasing trend from 2010 to 2018.
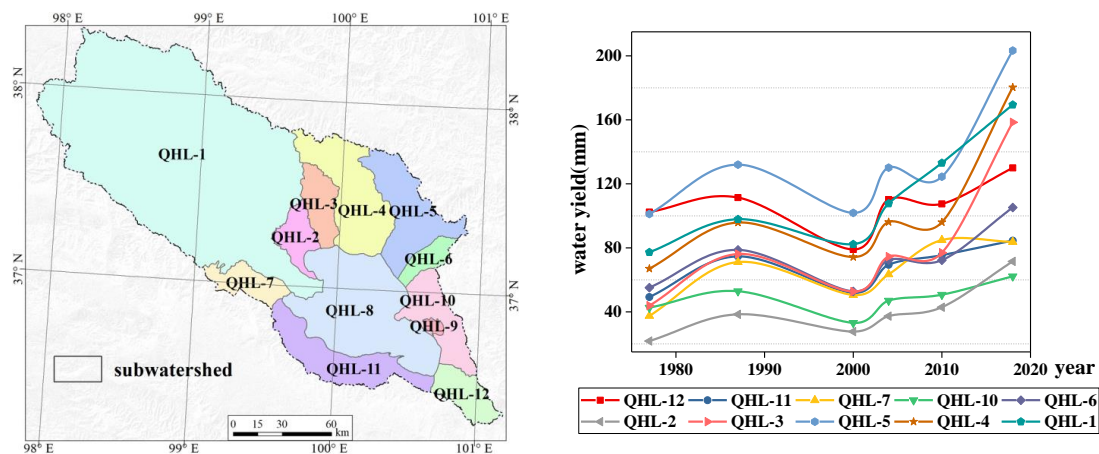

Figure 5. Sub-watershed and mean water yield of each sub-watershed (1977–2018).

As can be seen from the spatial distribution, the distribution of water yield had significant spatial heterogeneity. The spatial pattern of high and low values of water yield distribution was basically consistent during 1977 to 2018. Water yield increased gradually from southeast to northwest. We can find that areas of low water yield were mainly concentrated in the surrounding area of Qinghai lake. Water yield in mountain area was obviously more than that in the surrounding area of Qinghai lake. Areas with high water yield were located in the northern, western mountainous areas and edge of the watershed, especially in the central part of Tianjun county. Regional water yields showed an obvious increasing trend in Tianjun County and Gangcha County between 1977 and 2018. Water yield was very high in the area of alpine tundra. Water yields fluctuated between 0 mm and 780.68 mm in study area. The maximum water yield in 2018 was abnormally higher than before (Figure 6). In fact, the

population was mainly concentrated in the surrounding area of Qinghai lake. In contrast, areas with high water yield had less population distribution.
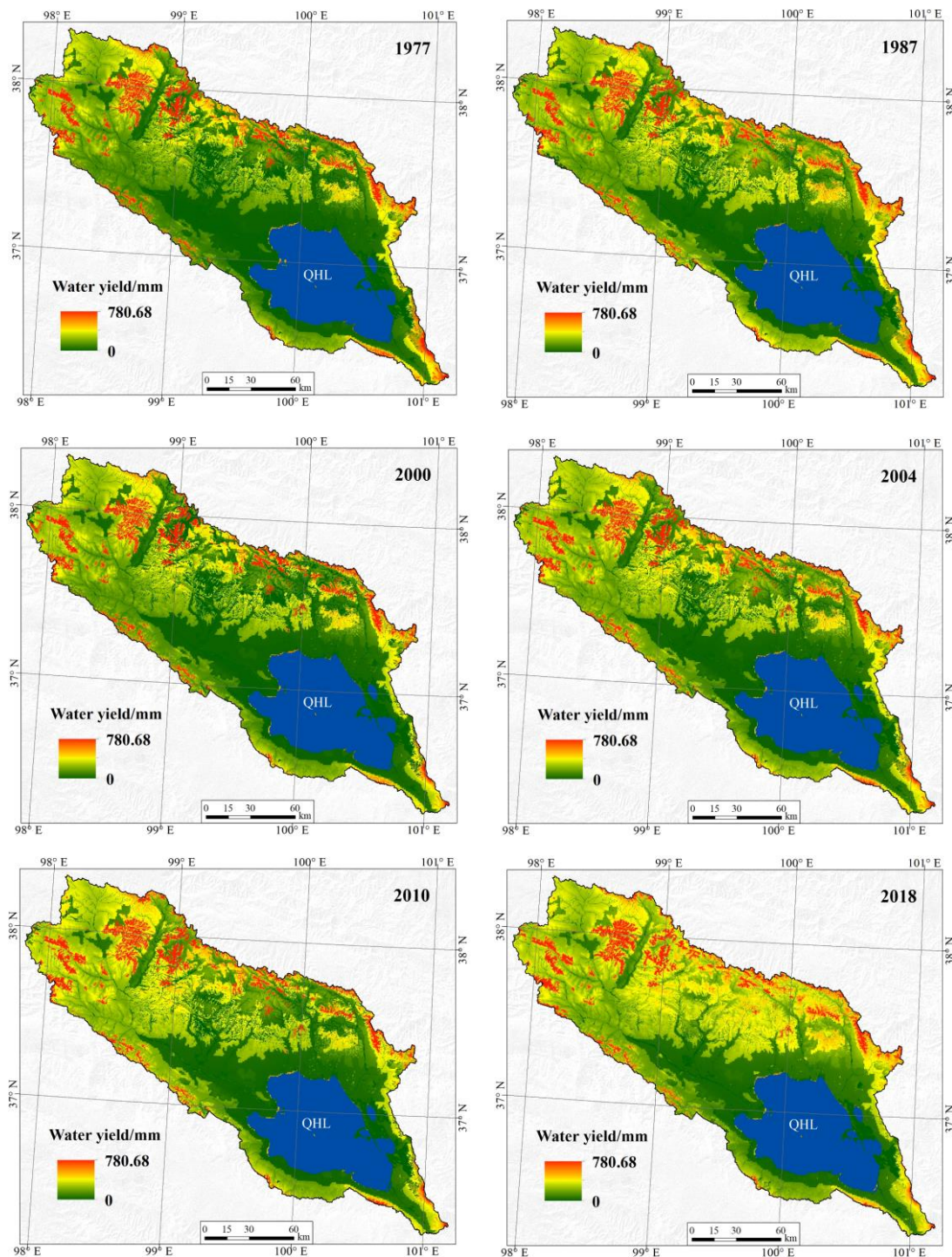

Figure 6. Spatial distribution of Water yield in Qinghai lake watershed (1977–2018).

3.4. Effect of Precipitation on Water Yield

Meteorological stations we analyzed were mainly three meteorological stations within the Qinghai lake watershed and the nearby Haiyan station. The names of the meteorological stations are Tianjun station, Gangcha station, Haiyan station, and Jiang Xigou station, respectively. We calculated the cumulative annual precipitation for each station (Figure 7). We used the moving average method to fit

the data of each meteorological station, in order to reflect the detailed change characteristics. Then, the linear fitting method was utilized to find a line to show the overall trend of data changes. The results showed that, the annual precipitation of Tianjun station had fluctuated from 250 mm to 450 mm, with an overall upward trend since 1955. The highest annual precipitation was 563.6 mm, and the lowest annual precipitation was 211.6 mm. Annual precipitation of Gangcha station had fluctuated from 270 mm to 450 mm, with an overall upward trend. The highest annual precipitation was 572.3 mm, and the lowest annual precipitation was 260.0 mm. It should be pointed out that Haiyan station only had precipitation data since 1976. Minimum precipitation of Haiyan station was 248.2 mm, and the maximum value was 522.3 mm. It showed a general upward tendency. Although the data of Jiang Xigou station was rare, the precipitation data of Jiang Xigou station from 1973 to 1998 only showed a slow rising trend. The highest annual precipitation was 635.7 mm, and the lowest annual precipitation was 325.2 mm.
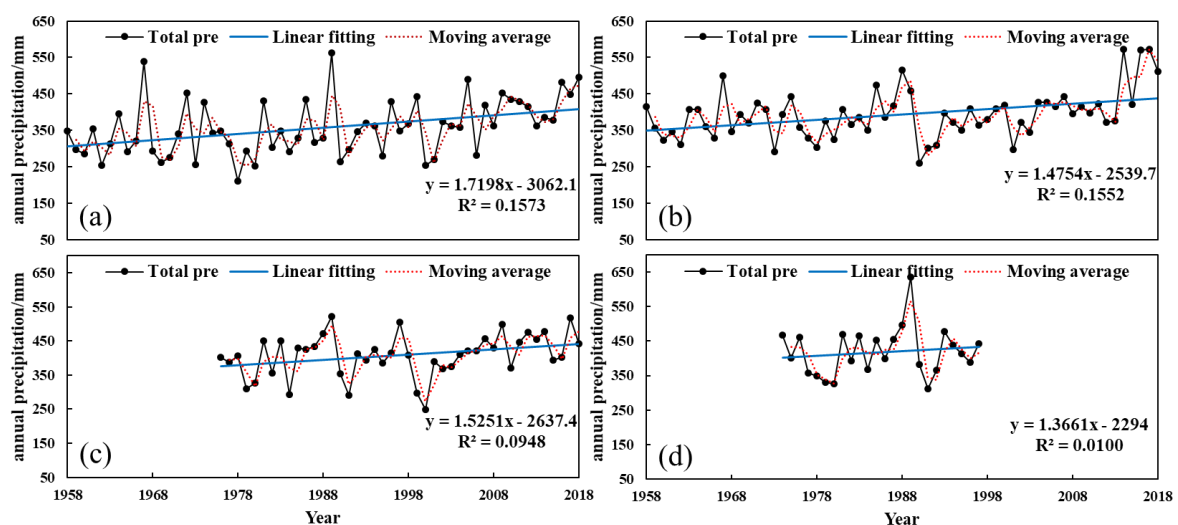

Figure 7. Annual precipitation of meteorological stations: (**a**) Tianjun station, (**b**) Gangcha station, (**c**) Haiyan station, and (**d**) Jiang Xigou station.

We calculated the average precipitation of the three meteorological stations in 1977, 1987, 2000, 2004, 2010, and 2018. Pearson correlation analysis was subsequently performed using these values and the annual water yields of the watershed. The results of this analysis indicated that the Pearson correlation coefficient between annual water yield and annual average precipitation was 0.954 ** (** correlation is significant at the 0.01 level), with a significance of 0.001. Taking regional variability into account, we carried out the Pearson correlation analysis on the annual precipitation of each station and the water yield of the sub-watershed where the station was located. It turned out that the Pearson correlation coefficient between annual water yield and annual precipitation was 0.899 * (* correlation is significant at the 0.05 level), with a significance of 0.006 in Tianjun station. And the Pearson correlation coefficient was 0.929 **, with a significance of 0.002. When precipitation changed with time period, water yield of the watershed also changed significantly, and there was a high correlation between the two variables. Therefore, precipitation became a very important factor which affected the changes of water yield.

Geographical distribution of the ratio of water yield to precipitation, which can reflect the consistency between the two, is showed in Figure 8. Comparing the spatial distribution of water yield depth per pixel to annual precipitation, the water yield rises with high precipitation. It can be seen from the spatial and temporal dynamic changes of the ratio of water yield to precipitation that precipitation had a high contribution rate to water yield. For instance, in 2018, the highest water yield was located in the northern, western mountainous areas (Figure 6). The ratio of water yield to precipitation also tended to be the highest in the same places, correspondingly (Figure 8).
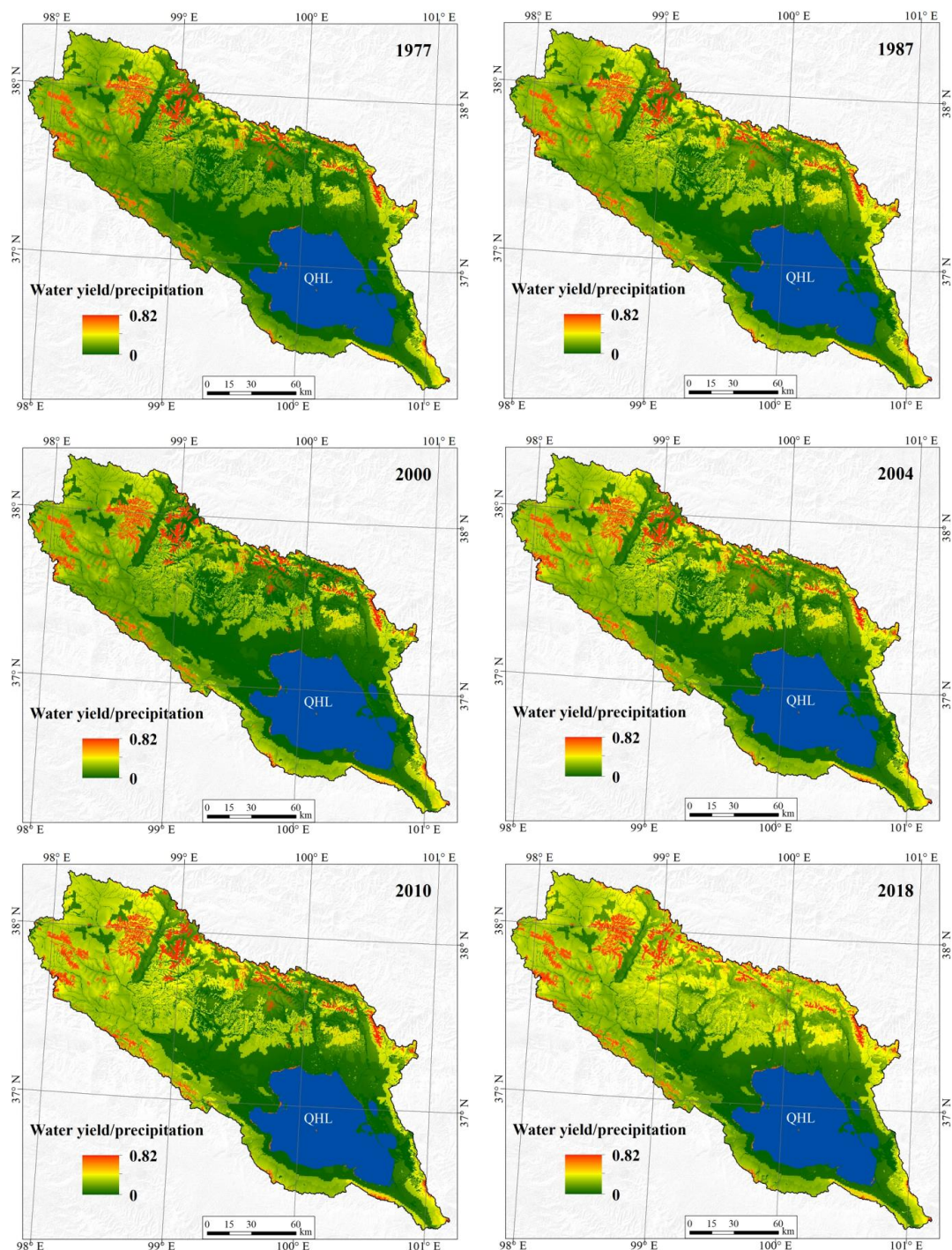
Figure 8. Spatial distribution of the ratio of water yield to precipitation in Qinghai lake watershed (1977–2018).

3.5. Effect of LUCC on Water Yield

The Pearson correlation was carried out to study the influence of LUCC on the changes of water yield (Table 5). The 22 LUCC classes were aggregated into six land cover types for each year. The Pearson correlation coefficients were calculated between changes of water yield and changes of cultivated land, forestland, grassland, water area, built-up land, and unused land. The highest positive correlation was observed between the change of water yield and the change of built-up land area, and the correlation coefficient was 0.932 *. The Pearson correlation coefficient between changes of water yield and changes of built-up land was 0.897 *. It should be noted that the changes of water yield were negatively correlated

with the changes of unused land and cultivated land. In conclusion, the change in the forestland, built-up land and unused land made major contribution to the change in the water yield.

Table 5. Pearson correlation between the changes of water yield and LUCC.

LUCC	Correlation	Significance
Cultivated land	−0.198	0.750
Forestland	0.897 *	0.039
Grassland	0.075	0.905
Water area	0.314	0.607
Built-up land	0.932 *	0.021
Unused land	−0.398	0.506

Note: * correlation is significant at the 0.05 level.

Figure 9 depicts the water yield in different LUCC types from 1977 to 2018. Overall, the water yield of each LUCC type showed an increasing trend. The mean and median of water yield of cultivated land were basically close from 1977 to 2010, and increased significantly in 2018. In fact, the area of cultivated land in 2018 declined slightly compared with 2010. The average water yield of forestland was 99 mm in 1977 and had been rising ever since. The mean water yield by forestland in 2018 was twice the average amount in 1977. The average water yield of grassland in 2018 was four times that of 1977. The lower quartile of water yield of grassland in 2018 was basically the same as the mean value in 2004. Grassland basically showed a downward trend, while the water yield of grassland increased. The mean and median of water area were close to 0. The water yield of built-up land increased significantly during 1977 to 1987. The average water yield of built-up land was approximately 50 mm and 100 mm, respectively, in 1977 and 1987. The variation range of water yield in 2000 was basically the same as that in 1987. The lower quartile and the upper quartile were similar to that in 1977, but the mean and median of water yield were both higher than that in 1977. Water yield of built-up land showed significant upward trend during 2000 to 2018. The lower quartile in 2004 was equal to the mean value in 2000. Compared with 2004, the lower quartile in 2010 was significantly higher, but the maximum was lower. The upper quartile in 2018 was approximately equal to the maximum in 2010, and the mean value and median were much higher than the upper quartile in 2010. The average water yield of unused land was basically above 115 mm, and the upper quartile was above 300 mm from 1977 to 2010, and the median was above 160 mm in 2018. The area of wetlands accounted for approximately 8.2% of the whole watershed. Wetlands which absorbed water during wet periods and released it during dry seasons could play an important role in hydrological process. In fact, water yield of wetlands was not high from 1977 to 2010, but increased in 2018. While, water yield of unused land increased from 1977 to 2018. In terms of spatial distribution, we found that the high value of water yield of unused land was mainly in the area of alpine tundra. The region of alpine tundra was less affected by human activities.
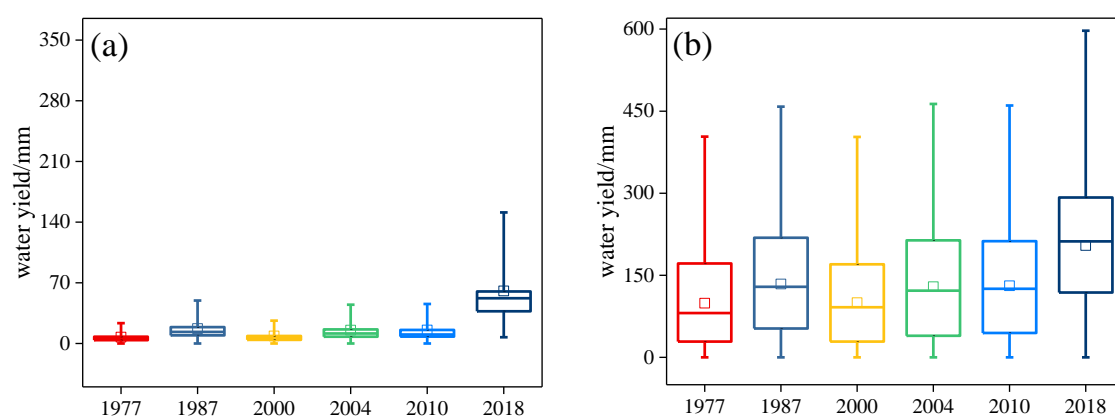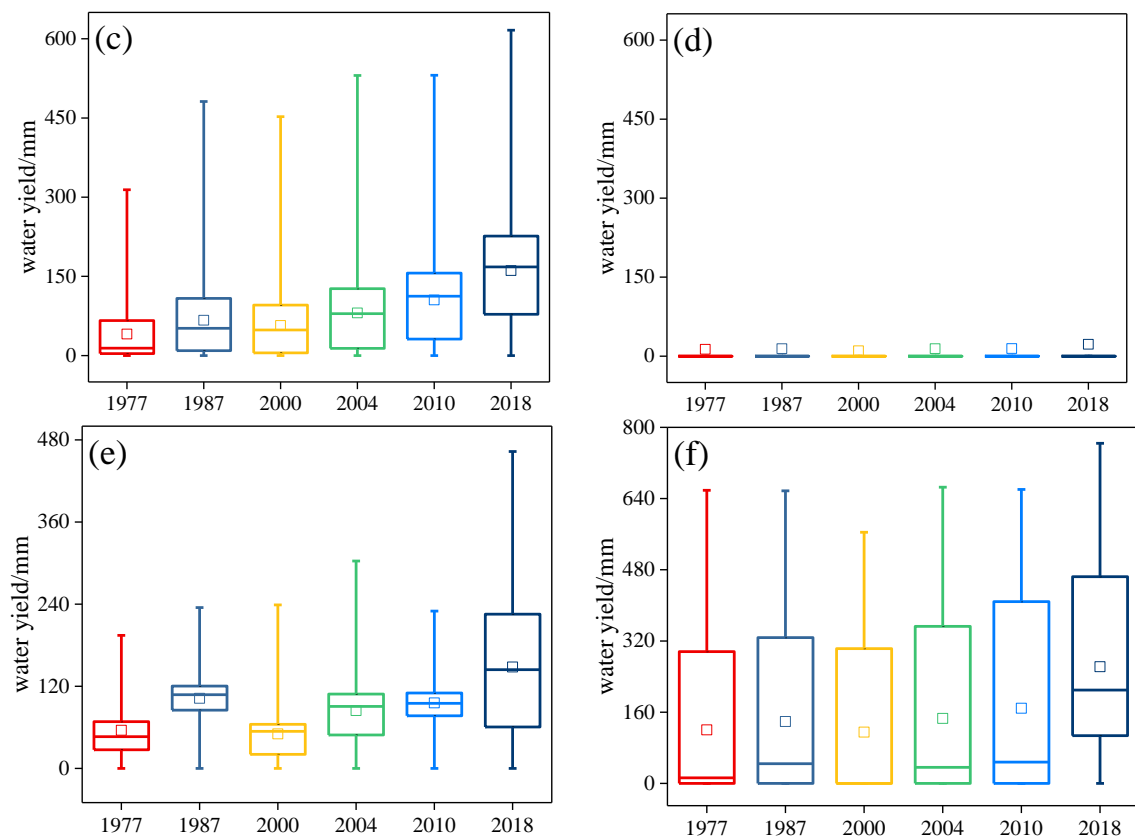

Figure 9. *Cont.*

Figure 9. Water yield in different LUCC types from 1977 to 2018. (**a**) Cultivated land, (**b**) forestland, (**c**) grassland, (**d**) water area, (**e**) built-up land and, (**f**) unused land.

3.6. Mechanism for LUCC and Climate Change Influencing Water Yield

LUCC and climate change are key drivers to the change of water yield in the Qinghai lake watershed. To further explore which factor is more significant for water yield changes in the study area, two different scenarios were designed: under the scenario without climate change and under the scenario without LUCC. Under the scenario without climate change, there was no change in the input meteorological data, which was always the meteorological data from 1977. However, the LUCC data in 1977, 1987, 2000, 2004, 2010, and 2018 were treated as the input data for the corresponding years. Under the scenario without LUCC, the LUCC conditions were assumed to be the same as 1977. Finally, the two scenarios and the actual conditions were compared to reveal the impacts of LUCC and climate change on water yield. It should be acknowledged that the impact of LUCC was far smaller than that of climate change (Table 6).

Table 6. Water yield under different scenarios.

Year	Only LUCC Scenario/10^8 m^3	Only Climate Change Scenario/10^8 m^3	Real Scenario/10^8 m^3
1977	18.17	18.17	18.17
1987	18.74	23.78	23.84
2000	19.64	18.81	19.03
2004	18.78	24.68	24.98
2010	18.33	28.54	28.97
2018	17.97	44.56	45.45

Under the scenario without LUCC, the water yield in the Qinghai lake watershed significantly increased, which was basically consistent with the real situation. Precipitation tends to quickly form runoff, which reduces soil moisture while increasing the water yield. Thus, precipitation directly

impacts the water yield. Under the scenario without climate change, the water yield showed an increasing trend and afterward a decreasing one.

To explore which one had the most impact on changes of water yield, the Pearson correlation was carried out between LUCC and the change of water yield under the scenario without climate change (Table 7). The highest positive correlation was observed between the change of water yield and the change of built-up land area, and the correlation coefficient was 0.979 **. The change of water yield was negatively correlated with the change of grassland and forestland, and the correlation coefficients were −0.952 * and −0.885 *, respectively. Correlation results indicate again that built-up land, grassland, and forestland made major contribution to the change in the water yield.

Table 7. Pearson correlation between the changes of water yield and LUCC (Only LUCC scenario).

LUCC	Correlation	Significance
Cultivated land	0.490	0.402
Forestland	−0.885 *	0.046
Grassland	−0.952 *	0.012
Water area	0.498	0.393
Built-up land	0.979 **	0.004
Unused land	0.617	0.267

Note: * correlation is significant at the 0.05 level, ** correlation is significant at the 0.01 level.

4. Discussion

LUCC can change the hydrological state of infiltration, evapotranspiration, and water retention [47]. The mechanism for LUCC influencing water yield was far more complex. Cultivated land had a capacity to hold the water in plants and soil. Meanwhile, crops need water to grow. During the stage from 1977 to 2000, the area of grassland decreased, which was consistent with the previous study [48]. Vegetation land produced lower water yield, because vegetated land had the ability to convert water into soil. This conclusion has been proved in existing studies [49,50]. Water yield of forestland increased, however, forestland decreased before 2010, and increased from 2010 to 2018. This was at odds with most previous studies [51], which suggested that forestland was responsible for the most water yield loss. A possible reason is that area of forestland in Qinghai lake watershed was only about 1.6% of the total area, and up to 85% of forest were sparse forest and shrubs, which have a lower water retention capacity. Built-up land is usually covered with asphalt, cement and concrete, forming an impermeable layer, which reduced the infiltration and concentration time [52]. Increases in built-up land led to increases in water yield. The conclusion was in line with the existing conclusions [53].

The finding that grassland and forestland produce lower water yield while built-up land generates more water yield was consistent with the existing studies [33,54]. But it is worth noting that the processes of LUCC are more complex. Meanwhile, conversions of LUCC lead to both negative and positive influence. Therefore, the overall consequence is not clear. In contrast, climate change is straightforward, but requires a long time to have a noticeable impact.

However, our study still has some limitations. InVEST represents bio-physical processes in a simplified manner, the model assumes all water yield from a pixel reaches a point. So the model does not distinguish between surface and subsurface water. At the same time, the limited ability of the model accounts for intra- annual variation in water supply. The retention and transport of water are both neglect in the model. Therefore, it is necessary to make some further improvement in future research. Although with these uncertainties, the results of this study can still reflect the general tendency of water yield, and reveal the relationship between water yield and LUCC and climate change. It can provide some reference information for scientific management and utilization of water resources and conserving the ecological environment.

5. Conclusions

Water yield is an important component of ecosystem services, which is related to regional ecological security and sustainable development of resources. In this study, we evaluated the dynamic change of water yield in Qinghai lake watershed from 1977 to 2018, and verified the simulation results with the data published by Qinghai water resources department. We also explored the influence of precipitation and LUCC on the water yield.

Our results demonstrated that water yield of the whole watershed tended to increase from 18.17 $\times 10^8$ m^3 in 1977 to 45.45 $\times 10^8$ m^3 in 2018. The distribution of water yield had obviously spatial heterogeneity. The water yield of mountain area was larger than that of the surrounding lake area.

The results show that precipitation change and LUCC both had important influence on water yield during 1977 to 2018. Compared with land use/land cover change, precipitation played a more dominant role in affecting water yield. In particular, we focused on the specific impact of each individual LUCC type on the change of water yield. The water yield of each LUCC type showed an increasing trend. The change in the built-up land, forestland, and unused land made major contribution to the change in the water yield.

In conclusion, InVEST model has good applicability and performance in Qinghai lake watershed. There are still some uncertainties in the simulation, but the results provide decision foundation for the scientific management of water resources and ecological environment protection.

References

1. Costanza, R.; d'Arge, R.; de Groot, R.; Farber, S.; Grasso, M.; Hannon, B.; Limburg, K.; Naeem, S.; O'Neill, R.V.; Paruelo, J.; et al. The value of the world's ecosystem services and natural capital. *Nature* **1997**, *387*, 253–260. [CrossRef]
2. Wu, J.G. Landscape sustainability science: Ecosystem services and human well-being in changing landscapes. *Landsc. Ecol.* **2013**, *28*, 999–1023. [CrossRef]
3. Millennium Ecosystem Assessment. In *Ecosystems and Human Well-being: Synthesis*; Island Press: Washington, DC, USA, 2005; pp. 1–137.
4. Polasky, S.; Nelson, E.; Pennington, D.; Johnson, K.A. The impact of land-use change on ecosystem services, biodiversity and returns to landowners: A case study in the State of Minnesota. *Environ. Resour. Econ.* **2011**, *48*, 219–242. [CrossRef]
5. Gao, J.; Li, F.; Gao, H.; Zhou, C.; Zhang, X. The impact of land-use change on water-related ecosystem services: A study of the Guishui River basin, Beijing, China. *J. Clean Prod.* **2017**, *163*, S148–S155. [CrossRef]
6. Egoh, B.; Rouget, M.; Reyers, B.; Knight, A.T.; Cowling, R.M.; van Jaarsveld, A.S.; Welz, A. Integrating ecosystem services into conservation assessments: A review. *Ecol. Econ.* **2007**, *63*, 714–721. [CrossRef]
7. Cudennec, C.; Leduc, C.; Koutsoyiannis, D. Dryland hydrology in Mediterranean regions—A review. *Hydrol. Sci. J.* **2007**, *52*, 1077–1087. [CrossRef]
8. Yang, D.; Liu, W.; Tang, L.; Chen, L.; Li, X.; Xu, X. Estimation of water provision service for monsoon catchments of South China: Applicability of the InVEST model. *Landsc. Urban Plan.* **2019**, *182*, 133–143. [CrossRef]
9. Ouyang, Z.; Zhu, C.; Yang, G.; Weihua, X.U.; Zheng, H.; Zhang, Y.; Xiao, Y. Gross ecosystem product: Concept, accounting framework and case study. *Acta Ecol. Sin.* **2013**, *33*, 6747–6761. [CrossRef]
10. Baker, T.J.; Miller, S.N. Using the Soil and Water Assessment Tool (SWAT) to assess land use impact on water resources in an East African watershed. *J. Hydrol.* **2013**, *486*, 100–111. [CrossRef]

11. Seppelt, R.; Dormann, C.F.; Eppink, F.V.; Lautenbach, S.; Schmidt, S. A quantitative review of ecosystem service studies: Approaches, shortcomings and the road ahead. *J. Appl. Ecol.* **2011**, *48*, 630–636. [CrossRef]

12. Redhead, J.W.; Stratford, C.; Sharps, K.; Jones, L.; Ziv, G.; Clarke, D.; Oliver, T.H.; Bullock, J.M. Empirical validation of the InVEST water yield ecosystem service model at a national scale. *Sci. Total Environ.* **2016**, *569*, 1418–1426. [CrossRef] [PubMed]

13. Hamel, P.; Guswa, A.J. Uncertainty analysis of a spatially explicit annual water-balance model: Case study of the Cape Fear basin, North Carolina. *Hydrol. Earth Syst. Sci.* **2015**, *19*, 839–853. [CrossRef]

14. Herman, J.D.; Kollat, J.B.; Reed, P.M.; Wagener, T. Technical note: Method of Morris effectively reduces the computational demands of global sensitivity analysis for distributed watershed models. *Hydrol. Earth Syst. Sci.* **2013**, *17*, 2893–2903. [CrossRef]

15. Geng, X.; Wang, X.; Yan, H.; Zhang, Q.; Jin, G. Land Use/Land Cover Change Induced Impacts on Water Supply Service in the Upper Reach of Heihe River Basin. *Sustainability* **2014**, *7*, 366–383. [CrossRef]

16. Donohue, R.J.; Roderick, M.L.; McVicar, T.R. Roots, storms and soil pores: Incorporating key ecohydrological processes into Budyko's hydrological model. *J. Hydrol.* **2012**, *436–437*, 35–50. [CrossRef]

17. Logsdon, R.A.; Chaubey, I. A quantitative approach to evaluating ecosystem services. *Ecol. Model.* **2013**, *257*, 57–65. [CrossRef]

18. Villa, F.; Bagstad, K.J.; Voigt, B.; Johnson, G.W.; Portela, R.; Honzak, M.; Batker, D. A methodology for adaptable and robust ecosystem services assessment. *PLoS ONE* **2014**, *9*, e91001. [CrossRef]

19. Hoyer, R.; Chang, H. Assessment of freshwater ecosystem services in the Tualatin and Yamhill basins under climate change and urbanization. *Appl. Geogr.* **2014**, *53*, 402–416. [CrossRef]

20. Mdk, L.; Matlock, M.D.; Cummings, E.C.; Nalley, L.L. Quantifying and mapping multiple ecosystem services change in West Africa. *Agric. Ecosyst. Environ.* **2013**, *165*, 6–18.

21. Zhang, C.; Li, W.; Zhang, B.; Liu, M. Water yield of Xitiaoxi river basin based on inVEST modeling. *J. Resour. Ecol.* **2012**, *3*, 50–54.

22. Su, C.; Fu, B. Evolution of ecosystem services in the Chinese Loess Plateau under climatic and land use changes. *Glob. Planet. Chang.* **2013**, *101*, 119–128. [CrossRef]

23. Yu, J.; Yuan, Y.; Nie, Y.; Ma, E.; Li, H.; Geng, X. The Temporal and Spatial Evolution of Water Yield in Dali County. *Sustainability* **2015**, *7*, 6069–6085. [CrossRef]

24. Song, W.; Deng, X.Z.; Yuan, Y.W.; Wang, Z.; Li, Z.H. Impacts of land-use change on valued ecosystem service in rapidly urbanized North China Plain. *Ecol. Model.* **2015**, *318*, 245–253. [CrossRef]

25. Legesse, D.; Vallet-Coulomb, C.; Gasse, F. Hydrological response of a catchment to climate and land use changes in Tropical Africa: Case study South Central Ethiopia. *J. Hydrol.* **2003**, *275*, 67–85. [CrossRef]

26. Cuo, L.; Beyene, T.K.; Voisin, N.; Su, F.; Lettenmaier, D.P.; Alberti, M.; Richey, J.E. Effects of mid-twenty-first century climate and land cover change on the hydrology of the Puget Sound basin, Washington. *Hydrol. Process.* **2011**, *25*, 1729–1753. [CrossRef]

27. Wang, C.; Hou, Y.; Xue, Y. Water resources carrying capacity of wetlands in Beijing: Analysis of policy optimization for urban wetland water resources management. *J. Clean. Prod.* **2017**, *161*, 1180–1191. [CrossRef]

28. Li, Q.F.; Cai, T.; Yu, M.X.; Lu, G.B.; Xie, W.; Bai, X. Investigation into the impacts of land-use change on runoff generation characteristics in the upper huaihe river basin, China. *J. Hydrol. Eng.* **2013**, *18*, 1464–1470. [CrossRef]

29. Woldesenbet, T.A.; Elagib, N.A.; Ribbe, L.; Heinrich, J. Hydrological responses to land use/cover changes in the source region of the Upper Blue Nile Basin, Ethiopia. *Sci. Total Environ.* **2017**, *575*, 724–741. [CrossRef]

30. Foley, J.A.; DeFries, R.; Asner, G.P.; Barford, C.; Bonan, G.; Carpenter, S.R.; Chapin, F.S.; Coe, M.T.; Daily, G.C.; Gibbs, H.K. Global consequences of land use. *Science* **2005**, *309*, 570–574. [CrossRef] [PubMed]

31. Qi, W.H.; Li, H.R.; Zhang, Q.F.; Zhang, K.R. Forest restoration efforts drive changes in land-use/land-cover and water-related ecosystem services in China's Han River basin. *Proc. Ecol. Eng.* **2019**, *126*, 64–73. [CrossRef]

32. Bossa, A.Y.; Diekkrüger, B.; Agbossou, E.K. Scenario-based impacts of land use and climate change on land and water degradation from the meso to regional scale. *Water* **2014**, *6*, 3152–3181. [CrossRef]

33. Li, S.; Yang, H.; Lacayo, M.; Liu, J.; Lei, G. Impacts of Land-Use and Land-Cover Changes on Water Yield: A Case Study in Jing-Jin-Ji, China. *Sustainability* **2018**, *10*, 960. [CrossRef]

34. Chang, B.; He, K.N.; Li, R.J.; Sheng, Z.P.; Wang, H. Linkage of Climatic Factors and Human Activities with Water Level Fluctuations in Qinghai Lake in the Northeastern Tibetan Plateau, China. *Water* **2017**, *9*, 552. [CrossRef]

35. Zheng, M.; Zhu, M.L.; Wang, Y.; Xu, C.; Yang, H. Eco-environment status evaluation and change analysis of Qinghai based on national geographic conditions census data. *ISPRS J. Photogramm. Remote Sens.* **2018**, *XLII-3*, 2453–2457. [CrossRef]

36. Zhang, T.; Cao, G.; Cao, S.; Zhang, X.; Zhang, J.; Han, G. Dynamic assessment of the value of vegetation carbon fixation and oxygen release services in Qinghai Lake basin. *Acta Ecol. Sin.* **2017**, *37*, 79–84. [CrossRef]

37. Zhang, T.; Cao, G.C.; Cao, S.K.; Chen, K.L.; Shan, Z.X.; Zhang, J. Spatial-temporal characteristics of the vegetation net primary production in the Qinghai Lake Basin from 2000 to 2012. *J. Desert Res.* **2015**, *35*, 1072–1080.

38. Budyko, M.I. *Climate and Life*; Academic press: New York, NY, USA, 1974; pp. 217–243.

39. Wu, X.; Wang, S.; Fu, B.; Liu, Y.; Zhu, Y. Land use optimization based on ecosystem service assessment: A case study in the Yanhe watershed. *Land Use Policy* **2018**, *72*, 303–312. [CrossRef]

40. Zhang, L.; Dawes, W.R.; Walker, G.R. Response of mean annual evapotranspiration to vegetation changes at catchment scale. *Water Resour. Res.* **2001**, *37*, 701–708. [CrossRef]

41. Berti, A.; Tardivo, G.; Chiaudani, A.; Rech, F.; Borin, M. Assessing reference evapotranspiration by the Hargreaves method in north-eastern Italy. *Agric. Water Manag.* **2014**, *140*, 20–25. [CrossRef]

42. Allen, G.G.; Pereira, L.S.; Raes, D.; Smith, M. Crop Evapotranspiration: Guide Lines for Computing Crop Water Requirements. In *FAO Irrigation and Drainage Paper No. 56*; FAO: Rome, Italy, 1998; pp. 1–281.

43. Hu, Q.; Yang, D.; Wang, Y.; Yang, Y. Global correction and applicability evaluation of Hargreaves formula. *Adv. Water Sci.* **2011**, *22*, 160–167.

44. Zhou, W.; Liu, G.; Pan, J.; Feng, X. Distribution of available soil water capacity in China. *J. Geogr. Sci.* **2005**, *15*, 3–12. [CrossRef]

45. Food and Agriculture Organization (FAO); International Institute for Applied Systems Analysis (IIASA); International Soil Reference and Information Centre (ISRIC); Institute of Soil Science, Chinese Academy of Sciences (ISSCAS); Joint Research Centre (JRC). *Harmonized World Soil Database*, version 1.1; FAO: Rome, Italy; IIASA: Laxenburg, Austria, 2009.

46. Pessacg, N.; Flaherty, S.; Brandizi, L.; Solman, S.; Pascual, M. Getting water right: A case study in water yield modelling based on precipitation data. *Sci. Total Environ.* **2015**, *537*, 225–234. [CrossRef] [PubMed]

47. Sanchez-Canales, M.; Lopez Benito, A.; Passuello, A.; Terrado, M.; Ziv, G.; Acuna, V.; Schuhmacher, M.; Elorza, F.J. Sensitivity analysis of ecosystem service valuation in a Mediterranean watershed. *Sci. Total Environ.* **2012**, *440*, 140–153. [CrossRef] [PubMed]

48. Wang, J.H.; Tian, J.H.; Li, X.Y.; Ma, Y.J.; Yi, W.J. Evaluation of concordance between environment and economy in Qinghai Lake Watershed, Qinghai- Tibet Plateau. *J. Geogr. Sci.* **2011**, *21*, 949–960. [CrossRef]

49. Im, S.; Kim, H.; Kim, C.; Jang, C. Assessing the impacts of land use changes on watershed hydrology using MIKE SHE. *Environ. Geol.* **2008**, *57*, 231–239. [CrossRef]

50. Yang, C.G.; Yu, Z.B.; Hao, Z.C.; Lin, Z.H.; Wang, H.M. Effects of vegetation cover on hydrological processes in a large region: Huaihe river basin, China. *J. Hydrol. Eng.* **2013**, *18*, 1477–1483. [CrossRef]

51. Bi, H.; Liu, B.; Wu, J.; Yun, L.; Chen, Z.; Cui, Z. Effects of precipitation and landuse on runoff during the past 50 years in a typical watershed in Loess Plateau, China. *Int. J. Sediment Res.* **2009**, *24*, 352–364. [CrossRef]

52. Liu, Y.Y.; Zhang, X.N.; Xia, D.Z.; You, J.S.; Rong, Y.S.; Bakir, M. Impacts of land-use and climate changes on hydrologic processes in the qingyi river watershed, China. *J. Hydrol. Eng.* **2013**, *18*, 1495–1512. [CrossRef]

53. Lang, Y.; Song, W.; Zhang, Y. Responses of the water-yield ecosystem service to climate and land use change in Sancha River Basin, China. *Phys. Chem. Earth* **2017**, *101*, 102–111. [CrossRef]

54. Im, S.; Brannan, K.M.; Mostaghimi, S. Simulating hydrologic and water quality impacts in an urbanizing watershed. *J. Am. Water Resour. Assoc.* **2003**, *39*, 1465–1479. [CrossRef]